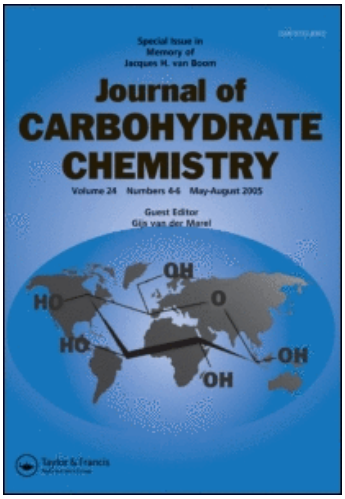

Journal of Carbohydrate Chemistry

Publication details, including instructions for authors and subscription information:
http://www.informaworld.com/smpp/title~content=t713617200

Conformational Study of α-*N*-Acetyl-D-Neuraminic Acid by Density Functional Theory

Toshihiko Sawada[a]; Tomohiro Hashimoto[b]; Hirofumi Nakano[c]; Mikiji Shigematsu[d]; Hideharu Ishida[d]; Makoto Kiso[d]

[a] The United Graduate School of Agricultural Science, Gifu University, Gifu, Japan [b] Faculty of Regional Studies, Gifu University, Gifu, Japan [c] Department of Chemistry, Aichi University of Education, Aichi, Japan [d] Department of Applied Bioorganic Chemistry, Faculty of Applied Biological Sciences, Gifu University, Gifu, Japan

To cite this Article Sawada, Toshihiko , Hashimoto, Tomohiro , Nakano, Hirofumi , Shigematsu, Mikiji , Ishida, Hideharu and Kiso, Makoto(2006) 'Conformational Study of α-*N*-Acetyl-D-Neuraminic Acid by Density Functional Theory', Journal of Carbohydrate Chemistry, 25: 5, 387 — 405

To link to this Article: DOI: 10.1080/07328300600778801

URL: http://dx.doi.org/10.1080/07328300600778801

Journal of Carbohydrate Chemistry, 25:387–405, 2006

ISSN: 0732-8303 print 1532-2327 online
DOI: 10.1080/07328300600778801

Conformational Study of α-*N*-Acetyl-D-Neuraminic Acid by Density Functional Theory

Toshihiko Sawada

The United Graduate School of Agricultural Science, Gifu University, Gifu, Japan

Tomohiro Hashimoto

Faculty of Regional Studies, Gifu University, Gifu, Japan

Hirofumi Nakano

Department of Chemistry, Aichi University of Education, Aichi, Japan

Mikiji Shigematsu, Hideharu Ishida, and Makoto Kiso

Department of Applied Bioorganic Chemistry, Faculty of Applied Biological Sciences, Gifu University, Gifu, Japan

The stable structures of α-*N*-acetyl-D-neuraminic acid (Neu5Acα) in the gas phase were studied at the B3LYP level of theory using 6-31G(d,p) and 6-31++G(d,p) basis sets. They are classified into five types according to the patterns of the intramolecular hydrogen bond formations. One of the stable structures had intramolecular hydrogen bond network of $O_9H_{O9}\cdots O_8H_{O8}\cdots O{=}C_1\text{-}O_1H_{O1}$ and $O_7H_{O7}\cdots O{=}CHN\text{-}C_5$ similar to the crystal structure of Neu5Ac-α-methyl glycoside methyl ester. The stable structures of Neu5Acα are reasonable for the following sialooligosaccharide ligand studies with respect to the relationship between OH group orientations and intramolecular hydrogen bond formations. The barrier heights for isomerizations between the stable structures were computed to be 2.8 to 6.7 kcal/mol at the B3LYP/6-31++G(d,p)// B3LYP/6-31G(d,p) level, which are basic factors for the conformational behavior of

Received February 20, 2006; accepted April 16, 2006.
Address correspondence to Toshihiko Sawada, The United Graduate School of Agricultural Science, Gifu University, 1-1 Yanagido, Gifu 501-1193, Japan. E-mail: tsawada@cc.gifu-u.ac.jp, and Makoto Kiso, Department of Applied Bioorganic Chemistry, Faculty of Applied Biological Sciences, Gifu University, 1-1 Yanagido, Gifu 501-1193, Japan. E-mail: kiso@cc.gifu-u.ac.jp

Neu5Acα before its interactions with receptors. We also calculated Neu5Acα−4 or 5-water complexes to take account of the solvent effect on the intramolecular hydrogen bonds in the stable structures. Consequently, the structures of Neu5Acα in the complexes are similar to each other, which is consistent with the known NMR data. Thus, the optimum Neu5Acα-water complexes are some of the reasonable pseudohydrous Neu5Acα.

Keywords *N*-acetylneuraminic acid, Conformation, Density functional theory, Hydrogen bond

INTRODUCTION

Sialylglycoconjugates such as gangliosides, sialic acid polymers, and mucin-type oligosaccharides on glycoproteins interact with various receptors in vivo. Sialyl Lewis^x (sLe^x) gangliosides[1] behave as ligands for E-, P-, and L-selectin belonging to a family of cell-adhesion molecules (C-type lectin).[2] The sLe^x-selectin interactions are concerned with gathering leukocyte and thrombocyte into inflammation site, permeation and metastasis of malignant cell, and so on.[3] Recently we reported the novel immune control system participated 6-sulfo-sLe^x (active),[4a,b] 6-sulfo-de-*N*-acetyl-sLe^x (super active),[4c−e] and 1,5-lactamized 6-sulfo-sLe^x (inactive)[4f−g] by human L-Selectin.[4h] Di- or tri-sialogangliosides GQ1bα, GT1aα, and GD1α are high reactive ligands for Siglec-4: sialic acid binding Ig like lectins-4 such as myelin-associated glycoprotein and schwann cell myelin protein.[5] α2-8 Polysialylated NCAM (neural cell adhension molecule) exists in a large quantity in the embryonic brain and active sites of adult brain.[6a] In adults, the polymerization degree drops off to α2-8 sialic acid dimer.[6b] Influenza A viruses strictly recognize nonreducing terminal disaccharide of sialylparaglobosides, in particular the sialic acid species and the difference in sialic acid-galactose linkage.[7a−b] Human influenza A virus hemagglutinin (HA) preferentially binds *N*-acetyl-D-neuraminic acid-α2 → 6-D-galactoseβ **1** (Neu5Acα2 → 6Galβ), but human HA mutation of Leu226 to glutamine binds Neu5Acα2 → 3Galβ **2** stronger than Neu5Acα2 → 6Galβ **1** (Fig. 1).[7c] Moreover, mutation of the Ser228 to glycine changes the specificity from Neu5Acα2 → 3Galβ to *N*-glycolylneuraminic acidα2 → 3Galβ.[7d]

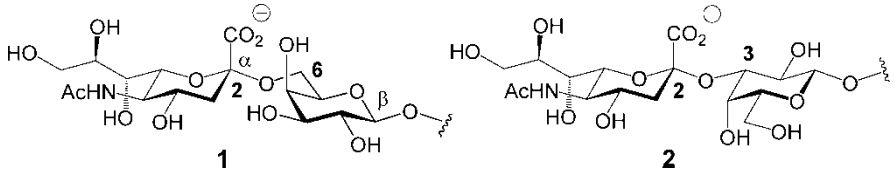

Figure 1: Nonreducing terminal disaccharides Neu5Acα2-6Galβ **1** and Neu5Acα2-3Galβ **2** recognized by influenza virus A hemagglutinin.

Recently the sialooligosaccharide-receptor interactions have been chemically elucidated by experimental methods such as X-ray crystal structure analysis[2c,8] and NMR experiments.[8a,9] These studies reported the interactions of sialooligosaccharide ligands with receptors in the crystal structures and experimental differences in sialooligosaccharide conformations between saccharide-bound receptor state and free state. But there is room for theoretical explanation of the interaction mechanisms. Our approach to quantitative clarification of sialooligosaccharide-receptor interaction mechanism is by two steps: Step 1: conformational studies of both a receptor and corresponding ligand before the interaction by theoretical calculations (reactant), and Step 2: a theoretical study of corresponding ligand-receptor complex based on the crystal structure (product).

Computational studies of sialooligosaccharide ligands were performed by molecular mechanics[8a,9d] and semi-empirical molecular orbital methods.[10] Hartree-Fock calculations were applied to monosaccharide α-*N*-acetyl-D-neuraminic acid (Neu5Acα) in order to discuss the interaction between the stable structure of Neu5Acα with neuraminidases or sialyltransferases.[11] However, we are interested in the hydrophilic and lipophilic interactions like the lectin-carbohydrate interaction, because electron correlation will be very significant to our sialooligosaccharide study. Besides, it is necessary to study the conformational behavior of Neu5Acα residue in terms of the relationships between the stable structures and several hydrogen bond formations before its interactions with receptors. Since oligosaccharides are too big and flexible for DFT studies, it is preferentially efficient to divide a sialooligosaccharide into monosaccharide units, optimize each unit, combine the optimum structure of nonreducing terminal unit and the optimum second unit, reoptimize a nonreducing terminal disaccharide, and repeat this method until making a target ligand.

In this paper, we report the stable structures in the gas phase and potential energy profile for isomerizations between the stable structures of

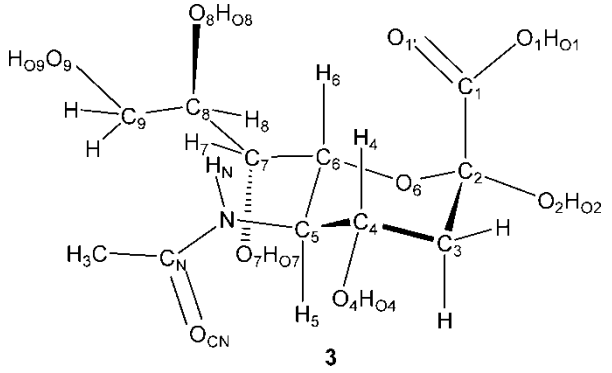

3

Figure 2: α-*N*-acetyl-D-neuraminic acid (Neu5Acα) **3**.

Neu5Acα **3** (Fig. 2) at the B3LYP level of theory using 6-31G(d,p) and 6-31++G(d,p) basis sets. We focus our attention on the relationships between the hydroxy group orientations in Neu5Acα and several hydrogen bond formations, which are assumed to be concerned with the sialooligosaccharide-receptor interaction as a part of ligand. Since Neu5Acα is practically hydrated in vivo, Neu5Acα can interact with solvent water molecules. We treat Neu5Acα-H_2O complexes as the pseudohydrous structures to investigate the effect of water molecules on the intramolecular hydrogen bonds in the gas phase structures.

METHODS

Eighty-one idealized C-OH bonds rotamers at the positions 4, 7, 8, and 9 of Neu5Acα **3** were studied by density functional theory calculations to search the relationships between the hydroxy group orientations and intramolecular hydrogen bond formations in the stable structures, since it is difficult to investigate hydroxy proton orientations of carbohydrates in aqueous system by experiments. First, we constructed the common structure of Neu5Acα **3** for the calculations referring to reported studies as follows[8a,12]: The six-membered ring conformation was set to be $^2C_5$ in our study because the experiments showed that the $^2C_5$ conformation was the most stable in water solution, and which was kept even after the interactions with selectins, influenza virus hemagglutinin, and siglecs. Dihedral angle of H_5-C_5-N-H_N was set to be 180° (Fig. 2). Glycerol side chain conformation was oriented to gauche-gauche (gg) at C_6-C_7 bond, trans (t) at C_7-C_8 bond, and gauche+ (g+) at C_8-C_9 bond, respectively (Sch. 1). The carboxy proton H_{O1} at position 1 was simply put on the oxygen atom O_1 referring to the crystal structure of Neu5Ac-α-methyl glycoside methyl ester (Neu5Acα-OMe CO_2Me).[13] Finally, anti (a), gauche+ (g+), and gauche- (g-) orientations of the hydroxy protons at the positions 4, 7, 8, and 9 with this basic structure gave the 81 initial rotamers for calculations ($3^4 = 81$, Sch. 2).

All initial rotamers were optimized at the RHF/3-21G(d) level in terms of all geometric parameters. Next, the optimum 14 structures within 4.0 kcal/mol

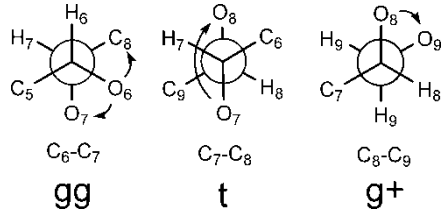

Scheme 1: Initial orientations at C_6-C_7, C_7-C_8, and C_8-C_9 bonds of Neu5Acα **3** for DFT calculations.

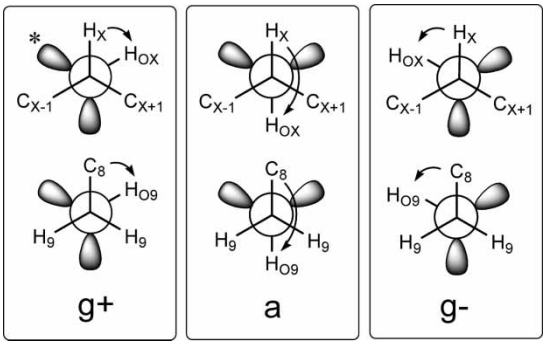

Scheme 2: C_X—O_XH_{OX} (X = 4, 7, 8) and C_9-O_9H_{O9} bonds rotamers of Neu5Acα **3** for DFT calculations. * The lobe is a lone pair on oxygen atom.

from the most stable structure were re-optimized at the B3LYP/6-31G(d,p) level[14] to take into account of electron correlation. Since previous works[15] have shown that diffuse functions are important for hydrogen-bonded systems in carbohydrates, some optimized structures at the B3LYP/6-31G(d,p) level were compared with those at B3LYP/6-31 + G(d) level. The difference between them was not significant for our system. For example, the hydrogen bond distances at the B3LYP/6-31 + G(d) level were about 0.04 Å longer than the corresponding B3LYP/6-31G(d,p) distances. Thus, we adopted 6-31G(d,p) set for the geometry optimizations for computational efficiency. Single-point energy calculations were also performed at the B3LYP level of theory using 6-31++G(d,p) basis sets. These methods are usual manners in comparison with those in the conformational study on methyl D-aldopentofuranosides by Houseknecht et al.[16] Vibrational frequency calculations were carried out at the B3LYP/6-31G(d,p) level with thermochemical corrections at 310 K and 1.0 atm. Consecutive isomerizations with respect to hydrogen bond conversions at one position between the stable conformers were also investigated at the B3LYP/6-31++G(d,p)//B3LYP/6-31G(d,p) level. Each transition state (Fig. 5) had one suitable imaginary frequency mode at the B3LYP/6-31G(d,p) level. In order to discuss the solvent effect on the stable structures, we intentionally put water molecules around the intramolecular hydrogen bonds in the stable structures and investigated the Neu5Acα-water complexes by the same theoretical methods, since some calculations with self-consistent reaction field models did not converge. The water molecules are considered to be the pseudo first hydration sphere here. All calculations were performed using GAUSSIAN 98[17] registered at Gifu University and Research Center for Computational Science, Okazaki Research Facilities, National Institutes of Natural Sciences. MOLDA[18] and MOLEKEL[19] were used to visualize the calculated results.

RESULTS AND DISCUSSION

Stable Structures of Neu5Acα

14 stable structures of Neu5Acα **3** at the B3LYP/6-31G(d,p) level almost kept the initial $^2C_5$ ring conformation and glycerol side chain conformation. Instead, the dihedral angle of H_5-C_5-N-H_N was changed to form intramolecular hydrogen bond with the OH group at the position 4 or 7, leading to more stable structures in the gas phase. The stable structures were classified into 5 types **A–E** according to the position of intramolecular hydrogen bond formations as described later. Figure 3 shows the most stable structures in each type, which are labeled as **A_4a**, **B**, **C_4a_9g+**, **D_9a**, and **E_9a**, respectively. Relative stabilities of the stable structures are summarized in Table 1.

Type **A** structures had hydrogen bond network $H_{O9} \cdots O_8 H_{O8} \cdots O_{1'}$ and $H_{O7} \cdots O_{CN}$. The O_4H_{O4} did not form intramolecular hydrogen bond. We labeled the type **A** structure having anti-orientation at 4-OH as **A_4a**, gauche+ as **A_4g+**, and gauche- as **A_4g−**. Structure **A_4a** was the most stable structure, and each hydrogen bond distance was $H_{O9} \cdots O_8 = 2.212$ Å,

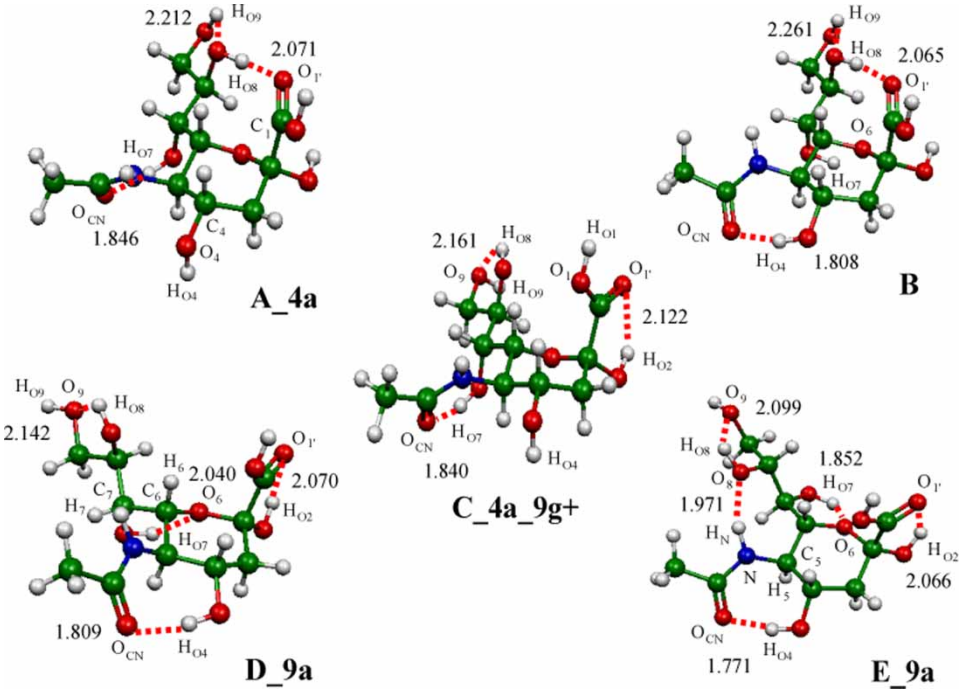

Figure 3: Stable structures **A_4a, B, C_4a_9 g+, D_9a**, and **E_9a** in the gas phase of Neu5Acα **3** at the B3LYP/6-31G(d,p) level. The red dotted lines are hydrogen bond interactions, which represent at angstrom (Å). Carbon, oxygen, nitrogen, and hydrogen atoms are represented as green, red, blue, and gray balls, respectively.

Table 1: Relative stabilities in kcal/mol for the stable structures of Neu5Acα **3**.

Entry	Structure	RHF/3-21G(d)	B3LYP/6-31G(d,p)		B3LYP/6-31++G(d,p)// B3LYP/6-31G(d,p)
		ΔE	ΔE	ΔG_{310}[a]	ΔE
1	**A_4a**	0.00	0.00	0.00	0.00
2	**A_4g+**	1.55	0.95	1.14	0.70
3	**A_4g−**	0.86	0.91	0.91	0.61
4	**B**	2.05	1.46	0.61	1.53
5	**C_4a_9g+**	2.16	1.34	1.09	0.60
6	**C_4a_9a**	2.17	2.51	2.58	1.19
7	**C_4g+_9g+**	3.68	2.57	3.28	1.57
8	**C_4g+_9a**	3.71	3.55	2.80	1.84
9	**C_4g−_9g+**	3.39	2.48	1.80	1.48
10	**C_4g−_9a**	3.43	3.41	2.52	1.67
11	**D_9a**	1.33	2.03	0.78	0.93
12	**D_9g+**	1.92	1.64	0.53	1.16
13	**E_9a**	−1.89	1.82	0.87	1.23
14	**E_9g+**	−1.20	1.47	0.80	1.58

[a] Thermochemical corrections were carried out at 310 K and 1.0 atm.

$H_{O8} \cdots O_{1'} = 2.071$ Å, and $H_{O7} \cdots O_{CN} = 1.846$ Å. Besides, hydroxy proton H_{O2} weakly interacted with the ring oxygen O_6 by the distance of 2.315 Å. Structures **A_4g+** and **A_4g−** were less stable than anti-conformer **A_4a** by 0.6–0.7 kcal/mol at the B3LYP/6-31++G(d,p)//B3LYP/6-31G(d,p) level (entry 2, 3).

Structure **B** had hydrogen bond network $H_{O9} \cdots O_8 H_{O8} \cdots O_{1'}$ similar to structure **A_4a**. The $H_{O9} \cdots O_8$ bond was longer by 0.05 Å than the corresponding bond in **A_4a**, while the $H_{O8} \cdots O_1$ bond length was almost the same. The carbonyl oxygen O_{CN} on acetamide group at position 5 formed a hydrogen bond with the hydroxy proton H_{O4}. The $H_{O4} \cdots O_{CN}$ bond length was 1.808 Å, which was shorter by 0.04 Å than the $H_{O7} \cdots O_{CN}$ bond in the **A_4a**. However, structure **B** was less stable than structure **A_4a** by 1.5 kcal/mol (entry 4). Hydroxy protons H_{O2} and H_{O7} weakly interacted with the ring oxygen O_6 with $H_{O2} \cdots O_6 = 2.360$ Å and $H_{O7} \cdots O_6 = 2.370$ Å.

Type **C** structures had three hydrogen bonds $H_{O2} \cdots O_{1'}$, $H_{O8} \cdots O_9$, and $H_{O7} \cdots O_{CN}$. The last one was common in both the type **A** and **C**, and the bond distances in these structures were similar. In the type **C**, the O_4H_{O4} and H_{O9} were not related with the hydrogen bond formations. Hydroxy proton H_{O9} preferred gauche+ or anti-orientation (entry 5–10). The most stable structure in this type was designated as **C_4a_9g+**, which had anti-orientation at 4-OH and gauche+ at 9-OH, and was less stable than structure **A_4a** by 0.6 kcal/mol at the B3LYP/6-31++G(d,p)//B3LYP/6-31G(d,p) level (entry 5). The hydrogen bond distances were $H_{O2} \cdots O_{1'} = 2.122$ Å, $H_{O8} \cdots O_9 = 2.161$ Å, and $H_{O7} \cdots O_{CN} = 1.840$ Å.

Type **D** structures had four hydrogen bonds $H_{O2} \cdots O_{1'}$, $H_{O8} \cdots O_9$, $H_{O4} \cdots O_{CN}$, and $H_{O7} \cdots O_6$. The first two were common with the type **C**, and the third was common with the type **B**. Hydroxy proton H_{O9} did not form an intramolecular hydrogen bond, so that the H_{O9} preferred gauche+ or anti-orientation similar to the type **C** (entry 11, 12). Structure **D_9a** was the most stable in the type **D** whose hydrogen bond distances were $H_{O2} \cdots O_{1'} = 2.070$ Å, $H_{O8} \cdots O_9 = 2.142$ Å, $H_{O4} \cdots O_{CN} = 1.809$ Å, and $H_{O7} \cdots O_6 = 2.040$ Å. The first two bonds were shorter than the corresponding bonds of **C_4a_9g+** by 0.02-0.05 Å. In spite of four hydrogen bond formations, structure **D_9a** was less stable than structures **A_4a** and **C_4a_9g+**, having three hydrogen bonds at the B3LYP/6-31++G(d,p)//B3LYP/6-31G(d,p) level (entry 11). Hydroxy proton H_{O7} was clearly interacted with the ring oxygen O_6, which caused orientation change at C_6-C_7 bond from the initial gg: $\angle H_6$-C_6-C_7-$H_7 = -60^\circ$ to -80°.

Type **E** structures were brought about by interaction of H_N with O_8H_{O8} in the **D** type structures. In structure **E_9a**, hydrogen bond network $H_N \cdots O_8H_{O8} \cdots O_9$ was generated to afford dihedral angles $\angle$ H_5-C_5-N-$H_N = -120^\circ$ and $\angle$ H_6-C_6-C_7-$H_7 = -119^\circ$, which caused the strong interactions $H_{O4} \cdots O_{CN} = 1.771$ Å and $H_{O7} \cdots O_6 = 1.852$ Å. However, structure **E_9a** was less stable than structure **D_9a** by 0.3 kcal/mol at the B3LYP/6-31++G(d,p)// B3LYP/6-31G(d,p) level (entry 13).

Table 1 shows that the order of relative stabilities of the most stable structures in each type is **A_4a** > **C_4a_9g+** > **B**, **E_9g +** > **D_9g+** at the B3LYP/6-31G(d,p) level. Since the relative stabilities at the RHF/3-21G(d) level are quite different from the corresponding stabilities at the B3LYP level, taking into account of electron correlation is very significant to our Neu5Acα study. The enlargement of the basis set to 6-31++G(d,p) reduced the energy gaps from the most stable **A_4a** except for **B** and **E_9g+**, and changed the order to **A_4a** > **C_4a_9g+** > **D_9a** > **E_9a** > **B**. Therefore, the diffuse functions strongly influenced **9a**-type structures than **9g+** type, leading to the reverse of the most stable structures in the type **D** and **E**. Table 1 also shows the relative Gibbs free energy at 310 K and 1.0 atm. Thermochemical correction did not change the most stable structure in each type, but the order was changed to **A_4a** > **D_9g+** > **B** > **E_9g+** > **C_4a_9g+**. The reduction of the ΔG mainly came from the entropy effect, which was the largest in the type **D**.

Lenthe et al. reported the stable structure of Neu5Acα at the HF/6-31G(d) level in order to discuss interaction of Neu5Acα with neuraminidases or sialyltransferases, which had intramolecular hydrogen bond network O_9 $H_{O8}O_8 \cdots H_{O1}OC_1$ and $H_{O7} \cdots O_{CN}$.[11] We were able to obtain this structure by migration of carboxy proton H_{O1} from O_1 to $O_{1'}$ in structure **C_4a_9g+** followed by interacting H_{O1} with $O_8H_{O8} \cdots O_9$ at the B3LYP/6-31G(d,p) level, so we labeled this one as **C_4a_9g+'** (Fig. 4). The distance of the

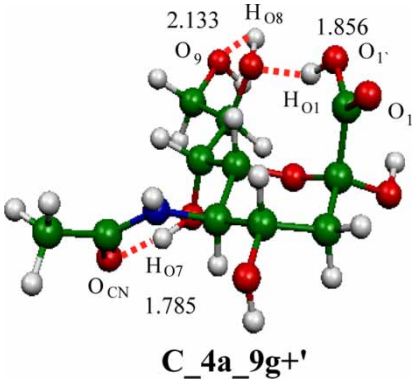

Figure 4: Stable structure **C_4a_9g+'** in the gas phase of Neu5Acα **3** at the B3LYP/6-31G(d,p) level.

$H_{O7} \cdots O_{CN}$ bond was 1.785 Å, which was shorter than the corresponding bond in **A_4a** by 0.06 Å. The hydrogen bond network $H_{O9}O_9 \cdots H_{O8}O_8 \cdots H_{O1}O_1{\cdot}C_1$ in **C_4a_9g+'** consisted of $H_{O9}O_9 \cdots H_{O8}O_8 = 2.133$ Å (**A_4a**; $O_9H_{O9} \cdots O_8H_{O8} = 2.212$ Å) and $H_{O8}O_8 \cdots H_{O1}O_1{\cdot}C_1 = 1.856$ Å (**A_4a**; $O_8H_{O8} \cdots O_1{\cdot}C_1 = 2.071$ Å). Therefore, structure **C_4a_9g+'** was more stable than structure **A_4a** by 0.65 kcal/mol at the B3LYP/6-31++G(d,p)//B3LYP/6-31G(d,p) level, and especially the hydrogen bond $O_8 \cdots H_{O1}$ contributed to the stabilization. However, these kinds of structures were not included in our initial target, because the position of the carboxy proton H_{O1} in structure **C_4a_9g+'** is different from the corresponding position of methyl group on CO_2Me in the crystal structure Neu5Acα-OMe CO_2Me.

Comparison between theoretical structure **A_4a** and crystal structure of Neu5Acα-OMe CO_2Me crystallized from methanol-ether[13] is summarized in Table 2. Structure **A_4a** was similar in hydroxy proton orientations and hydrogen bond distances to the crystal structure except for H_{O4} orientation and $H_{O9} \cdots O_8$ interaction. The O_4H_{O4} in the structures was not associated with intramolecular hydrogen bond formation, and the barrier height of the C_4-O_4H_{O4} bond rotation in structure **A_4a** was only 1.43 kcal/mol at the B3LYP/6-31++G(d,p)//B3LYP/6-31G(d,p) level. The distance of $H_{O9} \cdots O_8$ interaction in theoretical structure **A_4a** was shortened by 0.5 Å than corresponding distance in the crystal structure. The complex of Neu5Acα (**A_4a**) and water molecules designated as **wA_4a** had $H_{O9} \cdots O_8 = 2.789$ Å and $\angle$ C_8-C_9-O_9-$H_{O9} = -75^\circ$, which were similar to the corresponding parameters in the crystal structure.

These stable structures of Neu5Acα at the B3LYP/6-31G(d,p) level are reasonable for the following sialooligosaccharide ligand studies with respect to the relationship between OH group orientations and intramolecular hydrogen bond formations.

Table 2: Comparison between theoretical structure of Neu5Acα (**A_4a**) and crystal structure of Neu5Acα-OMe CO_2Me.

	Theoretical structure (B3LYP/6-31G(d,p))	**Crystal structure**
	Neu5Acα (A_4a)	**Neu5Acα-OMe CO_2Me**
Dihedral angle (degree)		
O_2-C_2-C_1-$O_{1'}$	84	108
H_4-C_4-O_4-H_{O4}	−178	110
H_5-C_5-N-H_N	134	142
H_7-C_7-O_7-H_{O7}	−39	−52
H_8-C_8-O_8-H_{O8}	−38	−41
C_8-C_9-O_9-H_{O9}	−47	−67
Distance (angstrom)		
$O_8H_{O8} \cdots O_{1'}C_1$	2.071	1.999
$O_9H_{O9} \cdots O_8H_{O8}$	2.212	2.705
$O_7H_{O7} \cdots O_{CN}C_NNH_N$	1.846	1.881

Isomerization Between the Stable Structures of Neu5Acα

The potential energy profile for the consecutive isomerizations between the structures **E_9a** and **B** in the gas phase at the B3LYP/6-31++G(d,p)//B3LYP/6-31G(d,p) level is shown in Figure 5. The transition state **TS1** for the isomerization between **E_9a** and **D_9a** (isomerization **E_9a**: $O_9 \cdots H_{O8}O_8 \cdots H_NN \leftrightarrow$ **D_9a**: $O_9 \cdots H_{O8}O_8$, H_NN) was located 0.02 kcal/mol above

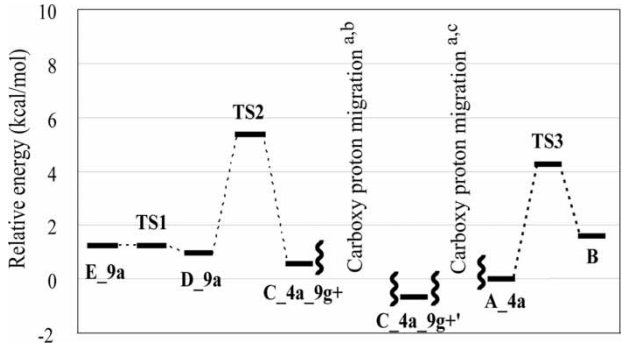

Figure 5: Potential energy profile for the isomerizations between the stable structures of Neu5Acα **3** at the B3LYP/6-31++G(d,p)//B3LYP/6-31G(d,p) level. [a] Carboxy proton H_{O1} migrations between O_1 to $O_{1'}$ required about 35 kcal/mol in the gas phase. The migrations can take place more easily in aqueous phase than C_1-C_2 bond rotations. We were not able to find corresponding transition states for the C_1-C_2 bond rotations. [b] Isomerization between ($O_9 \cdots H_{O8}O_8$, $H_{O1}O_{1'}C_1$) and ($O_9 \cdots H_{O8}O_8 \cdots H_{O1}O_{1'}C_1$: **C_4a_9g+'**). [c] Isomerization between (**C_4a_9g+'**: $H_{O9}O_9 \cdots H_{O8}O_8 \cdots H_{O1}O_{1'}C_1$) and ($O_9H_{O9} \cdots O_8H_{O8} \cdots O_{1'}(H_{O1})C_1$).

structure **E_9a**; thus, this isomerization was easier to take place in comparison with the others. It is known that density functional theories tend to underestimate barrier heights. In this work, this tendency was observed especially for **TS1**, which was computed to be 0.39 kcal/mol higher than **E_9a** at the B3LYP/6-31G(d,p) level. **TS1** had dihedral angles $\angle$ H_5-C_5-N-H_N = −121° and $\angle H_6$-C_6-C_7-H_7 = −95°, and distances $H_N \cdots O_8$ = 2.570 Å, $H_{O4} \cdots O_{CN}$ = 1.787 Å, and $H_{O7} \cdots O_6$ = 1.935 Å.

The conversion from hydrogen bond $H_{O4} \cdots O_{CN}$ to $H_{O7} \cdots O_{CN}$ (isomerizations **D_9a** → **C_4a_9g+** and **A_4a** ← **B**) required 4.41 kcal/mol at **TS2** and 2.77 kcal/mol at **TS3**, while the opposite conversions **D_9a** ← **C_4a_9g+** and **A_4a** → **B** needed 4.74 and 4.30 kcal/mol. **TS2** and **TS3** had $H_{O4} \cdots O_{CN}$ = 2.437 Å, 2.660 Å, $H_{O7} \cdots O_{CN}$ = 3.164 Å, 3.049 Å, and $\angle$ H_5-C_5-N-H_N = −175°, −179°.

The isomerizations between structure **C_4a_9g+**, **C_4a_9g+'**, and **A_4a** related to the carboxy proton H_{O1} migrations via 2 intermediates. These intermediates were stable structures at the B3LYP/6-31G(d,p) level; however, they were not found from the 81 initial structures. Carboxy proton H_{O1} migrations between O_1 and $O_{1'}$ can take place more easily in the aqueous phase. The transition state for isomerization between [$O_9 \cdots H_{O8}O_8$, $H_{O1}O_{1'}C_1$] and [O_9 $H_{O8}O_8 \cdots H_{O1}O_{1'}C_1$: **C_4a_9g+'**] was located 6.51 kcal/mol above structure **C_4a_9g+'**. The transition state for isomerization between [**C_4a_9g+'**: H_{O9} $O_9 \cdots H_{O8}O_8 \cdots H_{O1}O_{1'}C_1$] and [$O_9H_{O9} \cdots O_8H_{O8} \cdots O_{1'}(H_{O1})C_1$] was located 6.74 kcal/mol above stable structure **C_4a_9g+'**.

The main intramolecular hydrogen bonds conversions required 2.8 to 6.7 kcal/mol. This result is a basic factor for conformational behavior of Neu5Acα before its interaction with receptors in terms of the relationships between the stable structures and the hydrogen bond formations. The barrier heights will become lower in hydration system.

The Effect of Water Molecules on the Intramolecular Hydrogen Bonds in the Stable Structures of Neu5Acα

In order to discuss the effect of solvent water molecules on the intramolecular hydrogen bonds in the stable structures **A_4a**, **B**, **C_4a_9g+**, **D_9a**, **E_9a**, and **C_4a_9g+'**, each Neu5Acα-water complex was optimized at the B3LYP/6-31G(d,p) level. The optimized structures are shown in Figures 6 and 7. The complex **wA_4a** means the optimized structure obtained from the gas phase **A_4a** with solvent water molecules and others are designated in the same way. The complexes almost kept the $^2C_5$ ring conformation and glycerol side chain conformation. Instead, the intramolecular hydrogen bonds in the original gas phase structures were decomposed by insertion of 4 or 5 water molecules. The complexes **wD_9a** and **wC_4a_9g+'** had 4 solvent

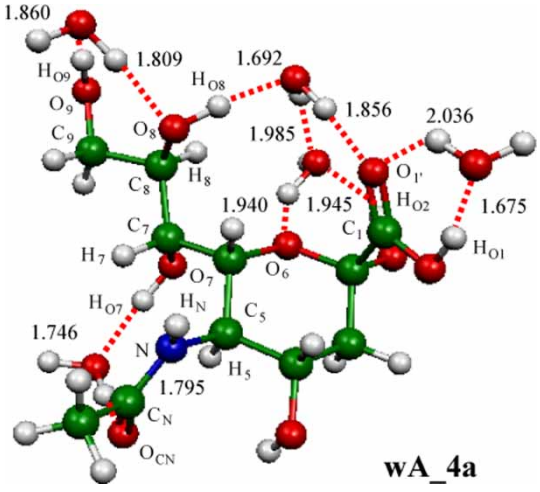

Figure 6: Optimum Neu5Acα-5 water complex **wA_4a** came from structure **A_4a** at the B3LYP/6-31G(d,p) level.

water molecules, while others had 5. They were assumed to be some of the pseudohydrous structures with pseudo first hydration sphere.

In complex **wA_4a**, water molecules interacted with the intramolecular hydrogen bonds $H_{O9} \cdots O_8 H_{O8} \cdots O_{1'} C_1$ and $H_{O7} \cdots O_{CN}$ in structure **A_4a**. One H_2O molecule was inserted into $H_{O9} \cdots O_8$ interaction to change the dihedral angle of C_8-C_9-O_9-H_{O9} from -47° to -75° and $H_{O9} \cdots O_8$ distance from 2.212 Å to 2.789 Å. These values were close to the corresponding parameters in the crystal structure of Neu5Acα-OMe CO_2Me. Complex **wA_4a** also had hydrogen bonds network $H_{O8} \cdots OH_2 \cdots O_{1'} C_1$, which supported the longhyphenrange interaction between H_{O8} and $O_{1'} C_1$ in polar solvent such as D_2O and Me_2SO-d_6 observed by nuclear overhauser effect. [8a,9c,20] By water molecules insertions, dihedral angles of H_5-C_5-N-H_N, H_7-C_7-O_7-H_{O7} and H_8-C_8-O_8-H_{O8} were changed from 134°, -39°, and -38° in the original structure **A_4a** to -177°, -14°, and -10°, respectively. Similar tendency was also seen in the other complexes **wB-wE_9a** and **wC_4a_9g+'** as shown in Figure 7.

The orientations of the carboxy group at position 1 in the theoretical structures and crystal structure of Neu5Acα-OMe CO_2Me are summarized in Table 3. Complexes **wA_4a** and **wB** had almost the same orientations as the crystal structure, and these dihedral angles of O_2-C_2-C_1-$O_{1'}$ were almost the same as those of the original gas phase structures **A_4a** and **B**. One of the solvent water molecules interacted with O_6, $O_{1'}$, and H_{O2} atoms in **wC_4a_9g+** and **wE_9a**, and the orientations of the carboxy group became closer to the corresponding orientation in Neu5Acα-OMe CO_2Me. In these four complexes having the similar orientation to the crystal

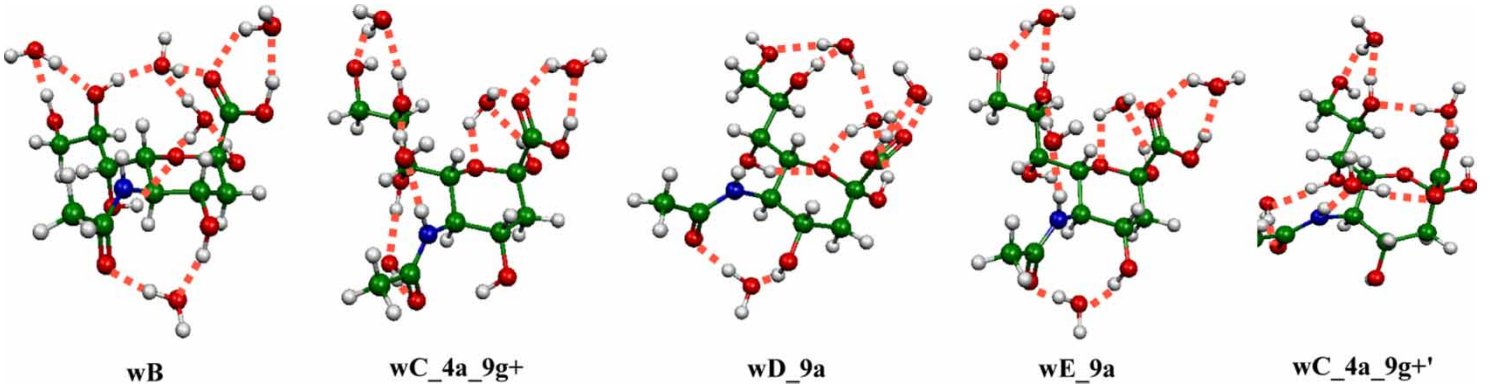

Figure 7: Neu5Acα-water complexes **wB, wC_4a_9 g+, wD_9a, wE_9a**, and **wC_4a_9g+'** came from the gas phase structures **B, C_4a_9 g+, D_9a, E_9a**, and **C_4a_9g+'** at the B3LYP/6-31G(d,p) level.

Table 3: Comparison between theoretical structures and crystal structure of Neu5Acα-OMe CO_2Me at dihedral angle of O_2-C_2-C_1-$O_{1'}$.

Structure	Dihedral angle (degree) O_2-C_2-C_1-$O_{1'}$
Neu5AcαOMe CO_2Me	108
A_4a// **wA_4a**	84// 83
B// **wB**	89// 92
C_4a_9g+// **wC_4a_9g+**	23// 72
D_9a// **wD_9a**	16// 31
E_9a// **wE_9a**	18// 76
C_4a_9g+'// **wC_4a_9g+'**	85// 55

structure, both $O_{1'}$ and H_{O1} atoms in the carboxy group interacted with the same solvent water molecule. On the other hand, complex **wD_9a** did not have these kinds of hydrogen bonds, and the deviation of the dihedral angle from the crystal structure was still large. Comparing the dihedral angles in the complex **wC_4a_9g+'** and the gas phase **C_4a_9g+'**, the latter orientation was much closer to the corresponding orientation in Neu5Acα-OMe CO_2Me.

Hydration energies in the Neu5Acα-water complexes were 13.3 to 14.3 kcal/mol per one water molecule at the B3LYP/6-31G(d,p) level. The structures of Neu5Acα in the complexes became similar to each other by the interactions of Neu5Acα with four or five water molecules. This result related to the NMR observation that there were few signals for the structural Neu5Acα isomer in water under normal condition.[8a] Besides, vicinal coupling constants based on the optimum Neu5Acα-water complexes are similar to corresponding experimental data (Table 4).[20a,21] Therefore, the optimum Neu5Acα-water complexes are some of the reasonable pseudohydrous Neu5Acα.

CONCLUSIONS

Eighty-one idealized C-OH bond rotamers of Neu5Acα were studied at the B3LYP level of theory using 6-31G(d,p) and 6-31++G(d,p) basis sets to afford 14 stable structures. According to intramolecular hydrogen bond or hydrogen bond network, they are classified into five types. The stable structure **A_4a** is similar to crystal structure of Neu5Acα-OMe CO_2Me. Since the relative stabilities of the stable structures at the RHF/3-21G(d) level are quite different from the corresponding stabilities at the B3LYP/6-31G(d,p) level, electron correlation has a large influence on the conformational study of Neu5Acα. The stable structures are reasonable for the following sialooligosaccharide ligand studies with respect to the relationship between OH group orientations and

Table 4: Vicinal coupling constants ($^3J_{H,\ H}$) in hertz for Neu5Acα.

	Experimental data		**Calculated data**[c]						
$^3J_{H,H}$	**Neu5Acα**		**A_4a**	**wA_4a**	**wB**	**wC_4a_9g+**	**wD_9a**	**wE_9a**	**wC_4a_9g+'**
3_{ax},4	11.8[a]		9.1	9.2	9.2	9.1	9.0	9.2	8.8
3_{eq},4	4.7[a]		2.4	2.0	1.6	2.5	2.6	2.0	3.4
4,5	10.4[a]		9.2	9.1	9.2	9.2	9.1	9.2	7.7
5,6	10.4[a]		9.2	8.6	8.5	9.2	9.2	9.1	7.7
6,7	0.8[a]	<2[b]	2.9	0.7	1.0	0.3	1.5	0.0	3.5
7,8	9.2[a]	8.5[b]	9.0	8.5	9.1	9.0	8.6	9.2	8.6
8,9S	2.5[a]	2.4[b]	2.2	0.8	0.8	0.4	0.5	0.6	0.4
8,9R	6.3[a]	5.9[b]	9.2	9.1	9.1	8.7	8.8	8.9	8.8

[a] Neu5Acα in D_2O.[21]
[b] Neu5Acα residue in GM1 ganglioside anchored in mixed D_2O/dodecylphosphocholine-d_{38} micelles.[20a]
[c] The data are given theoretically by the Karplus equations.

intramolecular hydrogen bond formations. The barrier heights of intramolecular hydrogen bond conversions between the stable structures of Neu5Acα were calculated to be 2.8 to 6.7 kcal/mol at the B3LYP/6-31++G(d,p)//B3LYP/6-31G(d,p) level, which are the basic factors for conformational behavior of Neu5Acα before its interactions with receptors. The Neu5Acα-water complexes were studied for a primary discussion of the solvent effect on the intramolecular hydrogen bonds. In the Neu5Acα-water complexes, four or five water molecules were inserted into the intramolecular hydrogen bonds. The structures of Neu5Acα in the complexes are similar to each other, which is consistent with the known NMR data. Thus, the optimum Neu5Acα-water complexes are some of the reasonable pseudohydrous Neu5Acα.

ACKNOWLEDGMENT

This work was supported in part by CREST, Japan Science and Technology Agency (JST), and a Grant-in-Aid (No. 17101007 to M. K.) for Scientific Research from Japan Society for the Promotion of Science.

REFERENCES

[1] (a) Kameyama, A.; Ishida, H.; Kiso, M.; Hasegawa, A. Synthetic studies on sialoglycoconjugates part 21. total synthesis of sialyl Lewis X. Carbohydr. Res. **1991**, *209*, c1–c4; (b) Kameyama, A.; Ishida, H.; Kiso, M.; Hasegawa, A. Synthetic studies on sialoglycoconjugates 22. Total synthesis of tumor-associated ganglioside, sialyl Lewis X. J. Carbohydr. Chem. **1991**, *10*, 549–560.

[2] (a) Tyrrel, D.; James, P.; Rao, N.; Foxall, C.; Abbas, S.; Dasgupta, F.; Nashed, M.; Hasegawa, A.; Kiso, M.; Asa, D.; Kidd, J.; Brandley, B.K. Structural requirements for the carbohydrate ligand of E-selectin. Proc. Natl. Acad. Sci. U.S.A. **1991**, *88*, 10372–10376; (b) Foxall, C.; Watson, S.R.; Dowbenko, D.; Fennie, C.; Lasky, L.A.; Kiso, M.; Hasegawa, A.; Asa, D.; Brandley, B.K. The three members of the selectin receptor family recognize a common carbohydrate epitope, the sialyl Lewisx oligosaccharide. J. Cell Biol. **1992**, *117*, 895–902; (c) Somers, W.S.; Tang, J.; Shaw, G.D.; Camphausen, R.T. Insights into the molecular basis of leukocyte tethering and rolling revealed by structures of P- and E-selectin bound to SLe(X) and PSGL-1. Cell **2000**, *103*, 467–479.

[3] (a) Lasky, L.A. Selectins: interpreters of cell-specific carbohydrate information during inflammation. Science **1992**, *258*, 964–969; (b) Varki, A. Selectin ligands. Proc. Natl. Acad. Sci. U.S.A. **1994**, *91*, 7390–7397; (c) McEver, R.P.; Moore, K.L.; Cummings, R.D. Leukocyte trafficking mediated by selectin-carbohydrate interactions. J. Biol. Chem. **1995**, *270*, 11025–11028.

[4] (a) Komba, S.; Ishida, H.; Kiso, M.; Hasegawa, A. Synthesis and biological activities of three sulfated sialyl Le(x) ganglioside analogues for clarifying the real carbohydrate ligand structure of L-selectin. Bioorg. Med. Chem. **1996**, *4*, 1833–1847; (b) Mitsuoka, C.; Sawada-Kasugai, M.; Ando-Furui, K.; Izawa, M.; Nakanishi, H.; Nakamura, S.; Ishida, H.; Kiso, M.; Kannagi, R. Identification of a major carbohydrate capping group of the L-selectin ligand on high endothelial venules in human lymph nodes as 6-sulfo sialyl Lewis X. J. Biol. Chem. **1998**, *273*, 11225–11233; (c) Galustian, C.; Lawson, A.M.; Komba, S.; Ishida, H.;

Kiso, M.; Feizi, T. Sialyl-Lewis(x) sequence 6-O-sulfated at N-acetylglucosamine rather than at galactose is the preferred ligand for L-selectin and de-N-acetylation of the sialic acid enhances the binding strength. Biochem. Biophys. Res. Commum. **1997**, *240*, 748–751; (d) Komba, S.; Galustian, C.; Ishida, H.; Feizi, T.; Kannagi, R.; Kiso, M. The first total synthesis of 6-sulfo-de-N-acetylsialyl Lewisx ganglioside: a superior ligand for human L-selectin. Angew. Chem. Int. Ed. **1999**, *38*, 1131–1133; (e) Komba, S.; Yamaguchi, M.; Ishida, H.; Kiso, M. 6-O-sulfo de-N-acetylsialyl Lewis X as a novel high-affinity ligand for human L-selectin: total synthesis and structural characterization. Biol. Chem. **2001**, *382*, 233–240; (f) Yamaguchi, M.; Ishida, H.; Kanamori, A.; Kannagi, R.; Kiso, M. Synthetic studies on sialoglycoconjugates Part 135. Studies on the endogenous L-selectin ligands: systematic and highly efficient total synthetic routes to lactamized-sialyl 6-O-sulfo Lewis X and other novel gangliosides containing lactamized neuraminic acid. Carbohydr. Res. **2003**, *338*, 2793–2812; (g) Hamada, T.; Hirota, H.; Yokoyama, S.; Yamaguchi, M.; Otsubo, N.; Ishida, H.; Kiso, M.; Kanamori, A.; Kannagi, R. NMR structure elucidation of cyclic sialyl 6-sulfo Lewis x, a biologically dormant form of L-selectin ligand. Tetrahedron Lett. **2003**, *44*, 1167–1170; (h) Mitsuoka, C.; Ohmori, K.; Kimura, N.; Kanamori, A.; Komba, S.; Ishida, H.; Kiso, M.; Kannagi, R. Regulation of selectin binding activity by cyclization of sialic acid moiety of carbohydrate ligands on human leukocytes. Proc. Natl. Acad. Sci. U.S.A. **1999**, *96*, 1597–1602.

[5] (a) Collins, B.E.; Ito, H.; Sawada, N.; Ishida, H.; Kiso, M.; Schnaar, R.L. Enhanced binding of the neural siglecs, myelin-associated glycoprotein and schwann cell myelin protein, to Chol-1 (α-series) gangliosides and novel sulfated Chol-1 analogs. J. Biol. Chem. **1999**, *274*, 37637–37643; (b) Sawada, N.; Ishida, H.; Collins, B.E.; Schnar, R.L.; Kiso, M. Ganglioside GD1α analogues as high-affinity ligands for myelin-associated glycoprotein (MAG). Carbohydr. Res. **1999**, *316*, 1–5; (c) Ishida, H.; Kiso, M. Synthetic study on neural siglecs ligands: systematic synthesis of α-series polysialogangliosides and their analogues. J. Synth. Org. Chem. Jpn. **2000**, *58*, 1108–1113; (d) Hara-Yokoyama, M.; Ito, H.; Ueno-Noto, K.; Takano, K.; Ishida, H.; Kiso, M. Novel sulfated gangliosides, high-affinity ligands for neural siglecs, inhibit NADase activity of leukocyte cell surface antigen CD38. Bioorg. Med. Chem. Lett. **2003**, *13*, 3441–3445; (e) Tsuchida, A.; Okajima, T.; Furukawa, K.; Ando, T.; Ishida, H.; Yoshida, A.; Nakamura, Y.; Kannagi, R.; Kiso, M.; Furukawa, K. Synthesis of disialyl Lewis a (Le^a) structure in colon cancer cell lines by a sialyltransferase, ST6GalNAc VI, responsible for the synthesis of α-series gangliosides. J. Biol. Chem. **2003**, *278*, 22787–22794.

[6] (a) Seki, T. Hippocampal adult neurogenesis occurs in a microenvironment provided by PSA-NCAM-expressing immature neurons. J. Neurosci. Res. **2002**, *69*, 772–783; (b) Sato, C.; Fukuoka, H.; Ohta, K.; Matsuda, T.; Koshino, R.; Kobayashi, K.; Troy, F.A.II.; Kitajima, K. Frequent occurrence of pre-existing alpha-2,8-linked disialic and oligosialic acids with chain lengths up to 7 sia residues in mammalian brain glycoproteins prevalence revealed by highly sensitive chemical methods and anti-di-, oligo-, and polysia antibodies specific for defined chain lengths. J. Biol. Chem. **2000**, *275*, 15422–15431.

[7] (a) Suzuki, Y.; Suzuki, T.; Takada, A.; Horimoto, T.; Wells, K.; Kida, H.; Otsuki, K.; Kiso, M.; Ishida, H.; Kawaoka, Y. Recognition of N-glycolylneuraminic acid linked to galactose by the α2,3 linkage is associated with intestinal replication of influenza A virus in ducks. J. Virol. **2000**, *74*, 9300–9305; (b) Suzuki, Y.; Ito, T.; Suzuki, T.; Holland, R.E., Jr.; Chambers, T.M.; Kiso, M.; Ishida, H.; Kawaoka, Y. Sialic acid species as a determinant of the host range of influenza A viruses. J. Virol. **2000**, *74*, 11825–11831; (c) Ito, T.; Suzuki, Y.; Takada, A.; Kawamoto, A.; Otsuki, K.; Masuda, H.; Suzuki, T.; Kida, H.; Kawaoka, Y. Differences in sialic acid-galactose linkages in the chicken egg amnion and allantois influence human influenza virus receptor specificity and variant selection. J. Virol. **1997**, *71*, 3357–3362;

(d) Masuda, H.; Suzuki, T.; Sugiyama, Y.; Horiike, G.; Murakami, K.; Miyamoto, D.; Jwa Hidari, K.I.; Ito, T.; Kida, H.; Kiso, M.; Fukunaga, K.; Ohuchi, M.; Toyoda, T.; Ishihama, A.; Kawaoka, Y.; Suzuki, Y. Substitution of amino acid residue in influenza A virus hemagglutinin affects recognition of sialyl-oligosaccharides containing N-glycolylneuraminic acid. FEBS. Lett. **1999**, *464*, 71–74.

[8] (a) Rao, V.S.R.; Qasba, P.K.; Balaji, P.V.; Chandrasekaran, R. *Conformation of Carbohydrates*; Harwood Academic Publishers: Netherlands, 1998; (b) Fotinou, C.; Emsley, P.; Black, I.; Ando, H.; Ishida, H.; Kiso, M.; Sinha, K.A.; Fairweather, N.F.; Isaacs, N.W. The crystal structure of tetanus toxin Hc fragment complexed with a synthetic GT1b analogue suggests cross-linking between ganglioside receptors and the toxin. J. Biol. Chem. **2001**, *276*, 32274–32281; (c) Merritt, E.A.; Kuhn, P.; Sarfaty, S.; Erbe, J.L.; Holmes, R.K.; Hol, W.G. 1.25 Å resolution refinement of the cholera toxin B-pentamer: evidence of peptide backbone strain at the receptor-binding site. J. Mol. Biol. **1998**, *282*, 1043–1059; (d) Emsley, P.; Fotinou, C.; Black, I.; Fairweather, N.F.; Charles, I.G.; Watts, C.; Hewitt, E.; Isaacs, N.W. The structures of the HC fragment of tetanus toxin with carbohydrate subunit complexes provide insight into ganglioside binding. J. Biol. Chem. **2000**, *275*, 8889–8894.

[9] (a) Cooke, R.M.; Hale, R.S.; Lister, S.G.; Shah, G.; Weir, M.P. The conformation of the sialyl lewis X ligand changes upon binding to E-selectin. Biochemistry **1994**, *33*, 10591–10596; (b) Scheffler, K.; Ernst, B.; Katopodis, A.; Magnani, J.L.; Wang, W.T.; Weisemann, R.; Peters, T. Determination of the bioactive conformation of the carbohydrate ligand in the E-selectin/sialyl Lewisx complex. Angew. Chem. Int. Ed. **1995**, *34*, 1841–1844; (c) Poppe, L.; Brown, G.S.; Philo, J.S.; Nikrad, P.V.; Shah, B.H. Conformation of sLex tetrasaccaride, free and bound to E-, P-, and L-selectin. J. Am. Chem. Soc. **1997**, *119*, 1727–1736; (d) Li, Y.T.; Li, S.C.; Hasegawa, A.; Ishida, H.; Kiso, M.; Bernardi, P.B.; Raimondi, L.; Sonnino, S. Structural basis for the resistance of Tay-sachs ganglioside GM2 to enzymatic degradation. J. Biol. Chem. **1999**, *274*, 10014–10018; (e) Bernardi, A.; Potenza, D.; Capelli, A.M.; García-Herrero, A.; Cañada, F.J.; Jiménez-Barbero, J. A three-dimensional view of their interactions with bacterial enterotoxins by nmr and computational methods. Chem. Eur. J. **2002**, *8*, 4597–4612; (f) Siebert, H.S.; André, S.; Lu, S.Y.; Frank, M.; Kaltner, H.; van Kuik, J.A.; Korchagina, E.Y.; Bovin, N.; Tajkhorshid, E.; Kaptein, R.; Vliegenthart, J.F.G.; von der Lieth, C.W.; Jiménez-Barbero, J.; Kopitz, J.; Gabius, H.J. Unique conformer selection of the human growth-regulatory lectin galectin-1 for ganglioside GM1 versus bacterial toxins. Biochemistry **2003**, *42*, 14762–14773.

[10] Pichierri, F.; Matsuo, Y. Effect of protonation of the N-acetyl neuraminic acid residue of sialyl lewisX: a molecular orbital study with insights into its binding properties toward the carbohydrate recognition domain of E-selectin. Bioorg. Med. Chem. **2002**, *10*, 2751–2757.

[11] van Lenthe, J.H.; den Boer, D.H.W.; Havenith, R.W.A.; Schauer, R.; Siebert, H.C. Ab initio calculations on various sialic acids provide valuable information about sialic acid-specific enzymes. J. Mol. Struct. (Theochem) **2004**, *677*, 29–37.

[12] Furuhata, K. Chemistry of N-acetylneuraminic acid (Neu5Ac). Trends Glycosci. Glycotechnol. **2004**, *16*, 143–169.

[13] Kooijman, H.; Kroon-Batenburg, L.M.J.; Kroon, J.; Breg, J.N.; de Boer, J.L. Structure of α-D-N-acetyl-1-O-methylneuraminic acid methyl ester. Acta. Cryst. Sect. C: Cryst. Struct. Commun. **1990**, *46*, 407–410.

[14] (a) Becke, A.D. Density-functional thermochemistry 3. The role of exact exchange. J. Chem. Phys. **1993**, *98*, 5648–5652; (b) Lee, C.; Yang, W.; Parr, R.G. Development

of the Colle-Salvetti correlation-energy formula into a functional of the electron density. Phys. Rev. B **1988**, *37*, 785–789.

[15] (a) Csonka, G.I.; Éliás, K.; Kolossváry, I.; Sosa, C.P.; Csizmadia, I.G. Theoretical study of alternative ring forms of α-L-fucopyranose. J. Phys. Chem. A **1998**, *102*, 1219–1229; (b) Lii, J.H.; Ma, B.; Allinger, N.L. Importance of selecting proper basis set in quantum mechanical studies of potential energy surfaces of carbohydrates. J. Comput. Chem. **1999**, *15*, 1593–1603.

[16] (a) Gordon, M.T.; Lowary, T.L.; Hadad, C.M. A computational study of methyl-α-D-arabinofuranoside: effect of ring conformation on structural parameters and energy profile. J. Am. Chem. Soc. **1999**, *121*, 9682–9692; (b) Houseknecht, J.B.; McCarren, P.R.; Lowary, T.L.; Hadad, C.M. Conformational studies of methyl 3-O-methyl-α-D-arabinofuranoside: an approach for studying the conformation of furanose rings. J. Am. Chem. Soc. **2001**, *123*, 8811–8824; (c) Houseknecht, J.B.; Lowary, T.L.; Hadad, C.M. Gas and solution phase energetics of the methyl α- and β-D-aldopentofuranosides. J. Phys. Chem. A **2003**, *107*, 5763–5777.

[17] Frisch, M.J.; Trucks, G.W.; Schlegel, H.B.; Scuseria, G.E.; Robb, M.A.; Cheeseman, J.R.; Zakrzewski, V.G.; Montgomery, J.A., Jr.; Stratmann, R.E.; Burant, J.C.; Dapprich, S.; Millam, J.M.; Daniels, A.D.; Kudin, K.N.; Strain, M.C.; Farkas, O.; Tomasi, J.; Barone, V.; Cossi, M.; Cammi, R.; Mennucci, B.; Pomelli, C.; Adamo, C.; Clifford, S.; Ochterski, J.; Petersson, G.A.; Ayala, P.Y.; Cui, Q.; Morokuma, K.; Malick, D.K.; Rabuck, A.D.; Raghavachari, K.; Foresman, J.B.; Cioslowski, J.; Ortiz, J.V.; Baboul, A.G.; Stefanov, B.B.; Liu, G.; Liashenko, A.; Piskorz, P.; Komaromi, I.; Gomperts, R.; Martin, R.L.; Fox, D.J.; Keith, T.; Al-Laham, M.A.; Peng, C.Y.; Nanayakkara, A.; Challacombe, M.; Gill, P.M.W.; Johnson, B.; Chen, W.; Wong, M.W.; Andres, J.L.; Gonzalez, C.; Head-Gordon, M.; Replogle, E.S.; Pople, J.A. Gaussian 98, Revision A.9. Gaussian, Inc: Pittsburgh, PA, 1998.

[18] (a) Ogawa, K.; Yoshida, H.; Suzuki, H. GRIMM - an interactive personal-computer graphics interface to molecular mechanics. J. Mol. Graphics. **1984**, *2*, 113–116; (b) Yoshida, H. Molecular structure data processor molda5. J. Assoc. Personal Computers Chemists **1986**, *8*, 45–68; (c) Yoshida, H.; Matsuura, H. MOLDA for windows - a molecular modeling and molecular graphics program using a vrml viewer on personal computers. J. Chem. Software. **1997**, *3*, 147–156.

[19] Flükiger, P.; Lüthi, H.P.; Portmann, S.; Weber, J. MOLEKEL 4.3, P. Swiss Center for Scientific Computing: Manno, Switzerland; 2000–2002.

[20] (a) Acquotti, D.; Poppe, L.; Dabrowski, J.; von der Lieth, C.W.; Sonnino, S.; Tettamanti, G. Three-dimensional structure of the oligosaccharide chain of GM1 ganglioside revealed by a distance-mapping procedure: a rotating and laboratory frame nuclear overhauser enhancement investigation of native glycolipid in dimethyl sulfoxide and in water-dodecylphosphocholine solutions. J. Am. Chem. Soc. **1990**, *112*, 7772–7778; (b) Poppe, L.; van Halbeek, H. Nuclear magnetic resonance of hydroxyl and amido, protons of oligosaccharides in aqueous solution: evidence for a strong intramolecular hydrogen bond in sialic acid residues. J. Am. Chem. Soc. **1991**, *113*, 363–365; (c) Siebert, H.C.; Reuter, G.; Schauer, R.; von der Lieth, C.W.; Dabrowski, J. Biochem. **1992**, *31*, 6962–6971; (d) Ichikawa, Y.; Lin, Y.C.; Dumas, D.P.; Shen, G.J.; Garcia-Junceda, E.; Williams, M.A.; Bayer, R.; Ketcham, C.; Walker, L.E.; Paulson, J.C.; Wong, C.H. Chemical-enzymic synthesis and conformational analysis of sialyl lewis x and derivatives. J. Am. Chem. Soc. **1992**, *114*, 9283–9298.

[21] Brown, E.B.; Brey, W., Jr.; Weltner, W., Jr. Cell-surface carbohydrates and their interactions 1 nmr of N-acetyl neuraminic acid. Biochim. Biophys. Acta. **1975**, *399*, 124–130.